Dissolution Behavior of SiO$_2$ and Electrochemical Reduction of Dissolved SiO$_2$ in Molten Chlorides

Y. Ma[a], T. Yamamoto[a], K. Yasuda[b, c, *], and T. Nohira[a]

[a] Institute of Advanced Energy, Kyoto University, Uji 611-0011, Japan
[b] Agency for Health, Safety and Environment, Kyoto 606-8501, Japan
[c] Graduate School of Energy Science, Kyoto University, Kyoto 606-8501, Japan
[*] Present address: Graduate School of Engineering, Kyoto University,
Kyoto 606-8501, Japan

To develop a new production process for SOG-Si with high productivity and low energy consumption, the structure of silicate ions in molten eutectic NaCl–CaCl$_2$ containing dissolved SiO$_2$ was investigated by Raman spectroscopy. The existence of SiO$_3^{2-}$ was indicated in melts containing 1.0 mol% of CaSiO$_3$ (O^{2-}/SiO$_2$ = 1.0). When 1.0 mol% of CaO was further added to the melt (O^{2-}/SiO$_2$ = 2.0), the existence of SiO$_4^{4-}$ was indicated. Cyclic voltammetry and potentiostatic electrolysis were conducted in molten NaCl–CaCl$_2$ with different silicate ions. From cyclic voltammograms, XRD analysis and SEM observation, silicate ions with different structure indicated different electrochemical reduction behavior; and the SiO$_3^{2-}$ ion is likely to be more suitable than SiO$_4^{4-}$ ion for the electrodeposition of Si.

Introduction

Photovoltaic (PV) power generation is considered as a source of clean and inexhaustible energy, which could substitute the conventional fossil-fuel power generation. The global production of PV cells achieved 102.4 GW in 2018, approximately 350 times the value in 2000 (1). Since crystalline silicon solar cells accounted for 96.9 % of the worldwide production in 2018 (2), they are expected to remain mainstream in the PV industry for the time being. Thus, the global demand for high-purity crystalline Si, which is known as solar-grade Si (SOG-Si), will also continue to increase in the future.

To develop a new production process for SOG-Si, experimental studies such as purification of metallurgical-grade silicon (3) and metallothermic reduction of silicon halides by metal reductants (4) have been conducted. Over the past two decades, we have been studying the electrochemical reduction of solid SiO$_2$ to Si in molten CaCl$_2$ to as a new production process for SOG-Si (5–7). In molten CaCl$_2$, electrochemical reduction of insulating SiO$_2$ proceeds by using a SiO$_2$ contacting electrode, which provides a three-phase interface of conductor/SiO$_2$/CaCl$_2$.

$$SiO_2(s) + 4\ e^- \rightarrow Si(s) + 2\ O^{2-} \qquad [1]$$
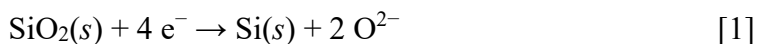
With the aim of efficient recovery of reduced Si, we also proposed an electrochemical reduction process of SiO$_2$ using a liquid Zn cathode in molten CaCl$_2$ (8–10). The overall process consists of three major steps: electrolysis, precipitation, and refining. In the

electrolysis step, solid SiO_2 is reduced to form Si–Zn liquid alloy. Then, solid Si is precipitated by decreasing the temperature of the liquid Si–Zn alloy in the precipitation step. The recovered Si is subjected to a refining step that comprises vacuum refining to remove residual Zn and directional solidification to manufacture SOG-Si ingots.

In our previous study, we found that direct electrochemical reduction of SiO_2 mainly occurred at the three-phase interface of $Zn/SiO_2/CaCl_2$. Although, the liquid Ca–Zn alloy, which formed at negative potentials, also contributed to the indirect reduction of SiO_2 below the $Zn/CaCl_2$ interface, i.e. in the liquid Zn cathode, the current efficiency was low since only part of Ca–Zn alloy contributed to the reduction of SiO_2 (10). In order to improve the productivity of the process, we focused on the electrochemical reduction of dissolved SiO_2, i.e., silicate ions (SiO_4^{4-}, SiO_3^{2-}, $Si_2O_5^{2-}$ etc.). When O^{2-} ion is added into molten salt, the dissolution of SiO_2 could be expressed as

$$x \, SiO_2(s) + y \, O^{2-} \rightarrow Si_xO_{(2x+y)}^{2y-}$$

[2]
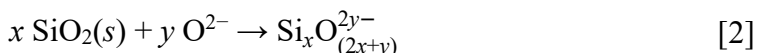
Electrodeposition of crystalline Si film from silicate ions has been reported by Bard and co-workers (11, 12). However, the structure of silicate ions has not been investigated.

In the present study, we focused on eutectic $NaCl–CaCl_2$, which has a lower melting point (777 K) than that of pure $CaCl_2$ (1045 K). The structure of silicate ions in molten eutectic $NaCl–CaCl_2$ with various concentrations of CaO was investigated by Raman spectroscopy. In our previous study, we have found that the structure of dissolved SiO_2 is identical to that of dissolved $CaSiO_3$ when the ratio of O^{2-}/SiO_2 is less than 1.0. Thus, $CaSiO_3$ was used as the source of SiO_3^{2-} ion, and CaO as the source of O^{2-} ion in this study. Also, electrochemical reduction of silicate ions was investigated at a solid graphite substrate, as the preliminary study for liquid Zn cathode.

Experimental

All experiments were conducted in a dry Ar atmosphere at 1023 K.

Structural Analysis of Silicate Ions by Raman Spectroscopy

NaCl and $CaCl_2$ powders (FUJIFILM Wako Pure Chemical Corp., reagent grade) were mixed in an eutectic composition ($NaCl:CaCl_2$ = 47.9:52.1 mol%), and then certain amounts of CaO (FUJIFILM Wako Pure Chemical Corp., reagent grade, 0 or 1.0 mol%) and $CaSiO_3$ (ALDRICH Chemistry, 200 mesh, 99%, 1.0 mol%) powders were added to the eutectic mixture. The mixture was loaded into a graphite crucible (Toyo Tanso Co., Ltd., IG-110 grade, o.d. 55 mm × i.d. 49 mm × height 150 mm) and dried under vacuum at 453 K for 2 days, then 723 K for 1 day. After the temperature was raised to 1023 K and maintained at that temperature for 1 day to sufficiently dissolve CaO and $CaSiO_3$, the salt was sampled by a Pyrex tube.

The sampled salt was then loaded into a Pt pan (Rigaku Corp., o.d. 5 mm × height 2.5 mm) and was placed in an air-tight high-temperature stage (Japan High Tech Co., Ltd., 10042). After the mixture was heated to 1023 K, the structure of silicate ions was investigated by Raman spectroscopy (Tokyo Instruments, Nanofinder 30). Figure 1 shows a schematic drawing of experimental apparatus for Raman spectroscopy.
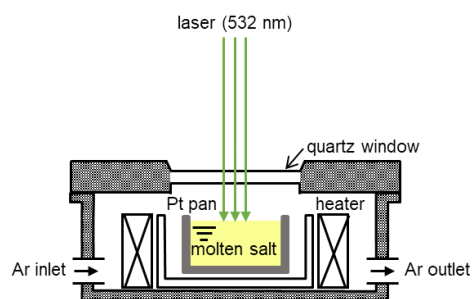
Figure 1. Schematic illustration of experimental apparatus for Raman spectroscopy of molten salt.

Electrochemical Reduction of Silicate Ions

NaCl and $CaCl_2$ powders were mixed in an eutectic composition and loaded into a graphite crucible (Toyo Tanso Co., Ltd., IG-110 grade, o.d. 80 mm × i.d. 70 mm × height 200 mm). The eutectic mixture was dried under vacuum at 453 K for 2 days and 723 K for 1 day. After the temperature was raised to 1023 K, certain amounts of CaO (0 or 1.0 mol%) and $CaSiO_3$ (1.0 mol%) powders were added to the eutectic mixture.

Figure 2 shows a schematic drawing of experimental apparatus for electrochemical reduction of silicate ions. As the working electrodes, a flag-like graphite plate (Toyo Tanso Co., Ltd., 3 mm × 3 mm × thickness 0.5 mm) was used for cyclic voltammetry and that with a size of 10 mm × 10 mm was used for electrolysis. The counter electrodes were glass-like carbon (Tokai Carbon Co., Ltd., diam.: 3.0 mm) for cyclic voltammetry and graphite square bar (Toyo Tanso Co., Ltd., 5 mm × 5 mm × height 50 mm) for electrolysis. A Si square bar (Furuuchi Chemical Corp., 5 mm × 5 mm × height 50 mm, 10 N) was used as the reference electrode.

The obtained samples were washed in a HCl solution (pH = 1) at 333 K and analyzed by X-ray diffraction (XRD, Rigaku, Ultima 4, Cu-$K\alpha$, λ = 1.5418 Å, 40 kV, 40 mA) and SEM (Phenom, Pro-SED).
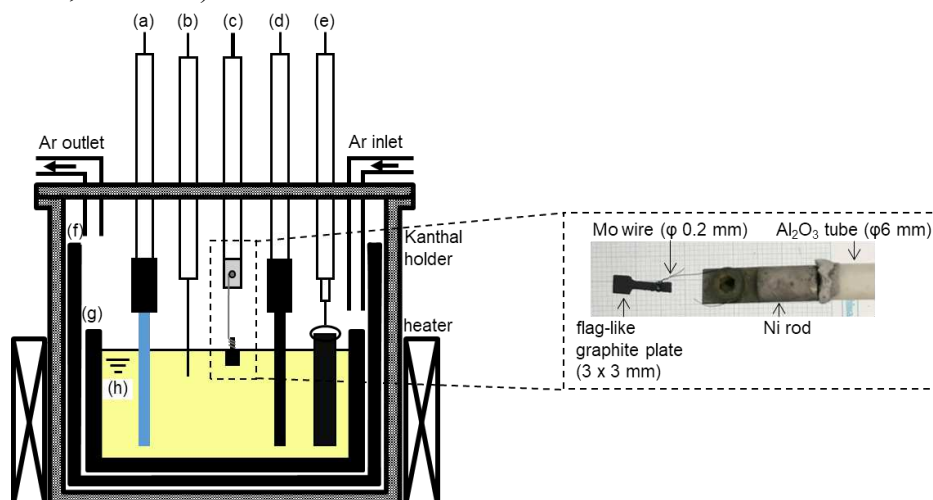

Figure 2. Schematic illustration of the electrolysis cell. (a) Si reference electrode, (b) Na^+/Na dynamic reference electrode on a Mo wire, (c) flag-like graphite working electrode, (d) glass-like carbon counter electrode, (e) graphite counter electrode, (f) graphite holder, (g) graphite crucible, and (h) molten NaCl–$CaCl_2$ containing CaO and $CaSiO_3$.

Results and Discussion

Structure of Silicate Ions

Figure 3 shows Raman spectra of molten (a) NaCl–CaCl$_2$–1.0 mol% CaSiO$_3$ and (b) NaCl–CaCl$_2$–1.0 mol% CaO–1.0 mol% CaSiO$_3$ at 1023 K. Within the wave number range of 700–1200 cm^{-1}, a strong band at 972 cm^{-1} and weak bands at 915, 1051 cm^{-1} were observed for molten salt (a). On the other hand, a strong band was detected at 830 cm^{-1} for molten salt (b). The main Raman bands for the stretch vibration of Si–O structures have been reported as 850–870 cm^{-1} for SiO$_4^{4-}$, 905–920 cm^{-1} for Si$_2$O$_7^{6-}$, 950–970 cm^{-1} for SiO$_3^{2-}$, and 1050–1100 cm^{-1} for Si$_2$O$_5^{2-}$, respectively (13–17). Therefore, the main structure is SiO$_3^{2-}$ in molten salt (a) and SiO$_4^{4-}$ in molten salt (b), which is consistent well with the O^{2-}/SiO$_2$ ratio in the melts. The weak bands of Si$_2$O$_7^{6-}$ and Si$_2$O$_5^{2-}$ ions are observed due to the disproportionation reaction of SiO$_3^{2-}$ ion (reaction [3]).

$$4 \ SiO_3^{2-} \rightarrow Si_2O_7^{6-} + Si_2O_5^{2-} \qquad\qquad [3]$$
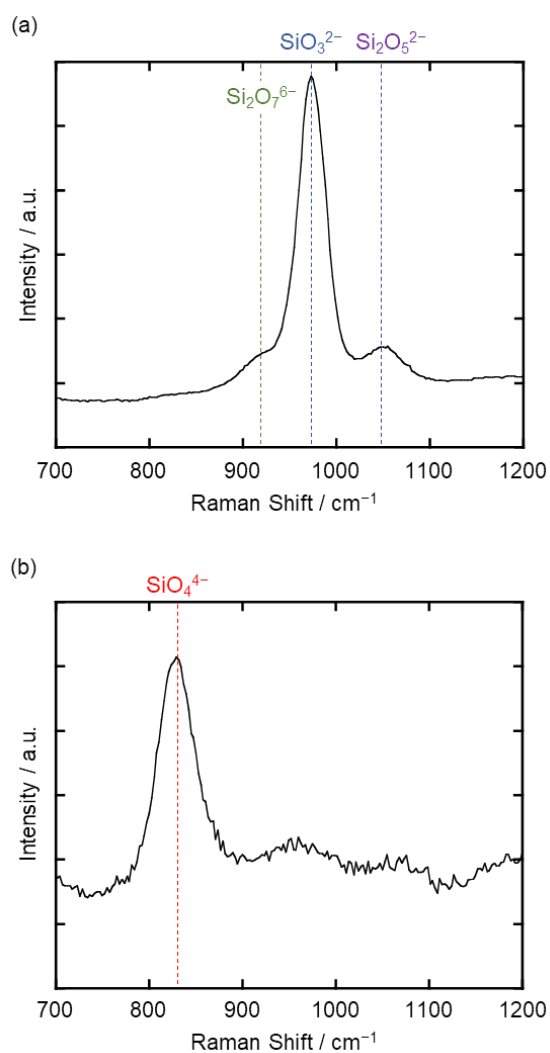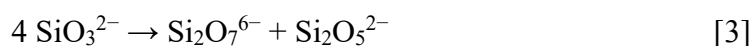

Figure 3. Raman spectra of molten NaCl–CaCl$_2$ containing (a) 1.0 mol% CaSiO$_3$, and (b) 1.0 mol% CaO–1.0 mol% CaSiO$_3$ at 1023 K.

Electrochemical Reduction of Silicate Ions

Figure 4 (a) shows cyclic voltammograms at a graphite electrode in molten NaCl–CaCl₂ before and after the addition of 1.0 mol% of CaSiO₃. The cathodic current observed in blank melt is likely due to the intercalation of Na or Ca metal into graphite. After the addition of CaSiO₃, cathodic currents increase from 1.2 V (vs. Na⁺/Na), suggesting the electrochemical reduction of SiO_3^{2-} ion. The sharp increase in cathodic current around 0.6 V is considered as the formation of Na–Si or Ca–Si alloy. Figure 4 (b) shows the voltammogram measured after the addition of 1.0 mol% of CaO and 1.0 mol% CaSiO₃. Cathodic currents were observed from the rest potential (1.8 V), which suggests the electrochemical reduction of SiO_4^{4-} ion. The sharp increase from 0.6 V is supposed to be the same as that for SiO_3^{2-} ion in Figure 4 (a).
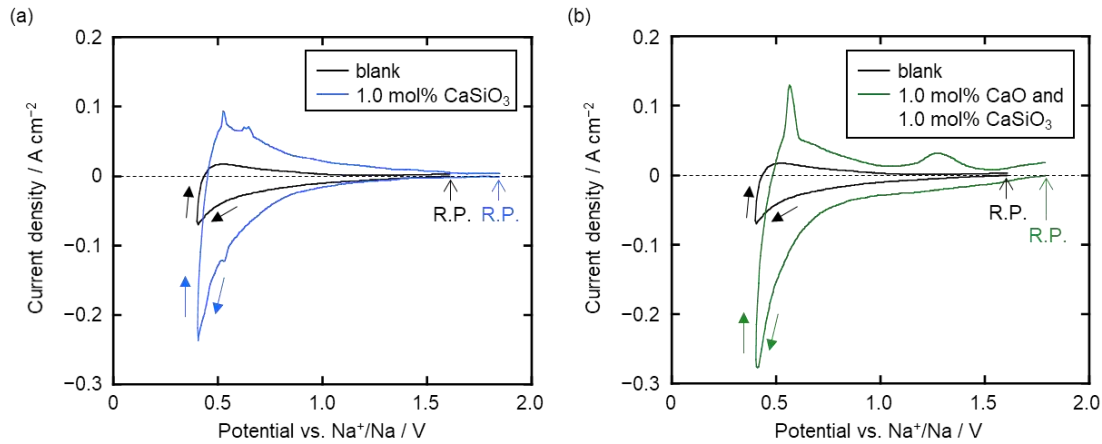

Figure 4. Cyclic voltammograms at a graphite electrode in molten NaCl–CaCl₂ before and after the addition of (a) 1.0 mol% of CaSiO₃, and (b) 1.0 mol% of CaO and 1.0 mol% of CaSiO₃ at 1023 K. Scan rate: 50 mV s⁻¹.

On the basis of the voltammetric results, potentiostatic electrolysis was conducted at 0.90, 0.70, and 0.50 V for −14 C cm⁻² in molten NaCl–CaCl₂ containing 1.0 mol% of CaSiO₃ (molten salt (a)), and 1.0 mol% of CaO and 1.0 mol% of CaSiO₃ (molten salt (b)). The optical images of the graphite substrate and electrolyzed samples are shown in Figure 5. For samples obtained in molten salt (a), small amount of deposits were observed at 0.90 V and 0.50 V, and quite amount of deposit in brown color at 0.70 V. For samples obtained in (b), no significant deposit was observed at 0.90 V, deposits in brown and gray colors were obtained at 0.70 V, and deposit in gray color at 0.50 V.

Figure 6 shows XRD patterns of a graphite substrate and the electrolyzed samples. For samples obtained at 0.90 and 0.70 V in molten salt (a), the formation of Si was confirmed, indicating that the increase in cathodic current from 1.2 V in Figure 4 (a) is the electrochemical reduction of SiO_3^{2-} ion to solid Si.

$$SiO_3^{2-} + 4 \text{ e}^- \rightarrow Si(s) + 3 \text{ O}^{2-} \tag{4}$$
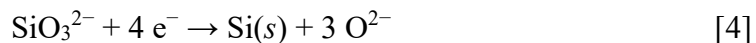
Since CaSi₂ was identified for the sample at 0.50 V, the sharp increase from 0.6 V corresponds the formation of CaSi₂.

$$2 \text{ Si}(s) + Ca^{2+} + 2 \text{ e}^- \rightarrow CaSi_2(s) \tag{5}$$
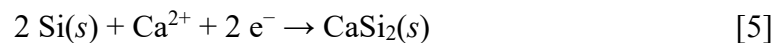
For samples obtained in molten salt (b), only graphite was detected at 0.90 V. The existence of Si was confirmed at 0.70 V, and both Si and $CaSi_2$ were detected at 0.50 V. Since Si deposition was only observed at potentials more negative than 0.70 V, the electrochemical reduction of SiO_4^{4-} ion to Si is considered to be more difficult than that of SiO_3^{2-} ion. Similarly, the formation of $CaSi_2$ seems to be less favorable for SiO_4^{4-} ion compared with SiO_3^{2-} ion.

Figure 7 shows surface SEM images of deposits. In molten salt (a), wire-like Si was obtained at 0.90 V and particle Si at 0.70 V. Dense $CaSi_2$ was observed at 0.50 V. For samples obtained in molten salt (b), wire-like Si was observed at 0.70 V and particle Si at 0.50 V.

From the results of XRD and SEM, the electrodeposition of Si from SiO_3^{2-} ion started from a more positive potential than that of SiO_4^{4-} ion. Thus, SiO_3^{2-} ion will be more suitable for the electrodeposition of Si at liquid Zn cathode as well as at solid graphite electrode.
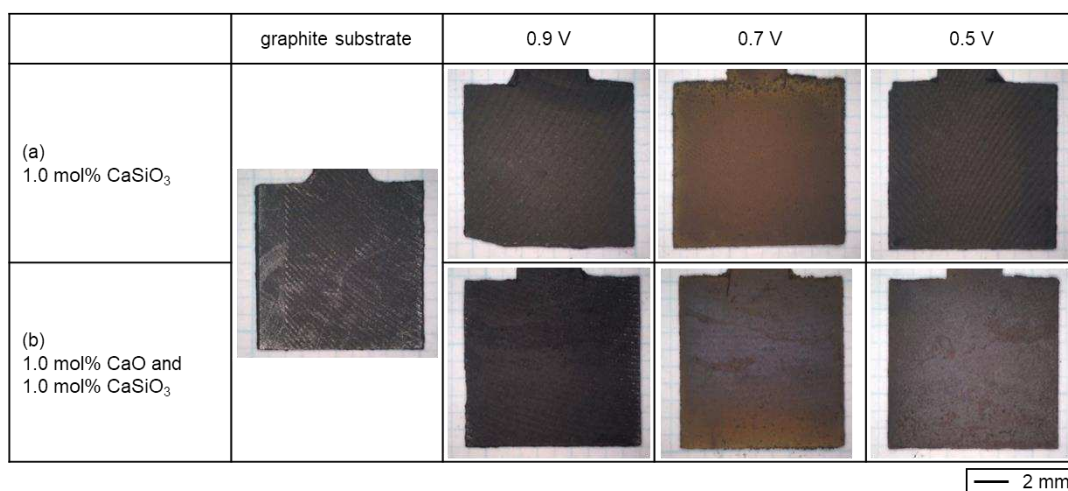

Figure 5. Optical images of the graphite substrate and samples obtained by electrolysis at graphite plates in molten $NaCl-CaCl_2$ containing (a) 1.0 mol% of $CaSiO_3$, and (b) 1.0 mol% of CaO and 1.0 mol% of $CaSiO_3$. Charge density: -14 C cm^{-2}.
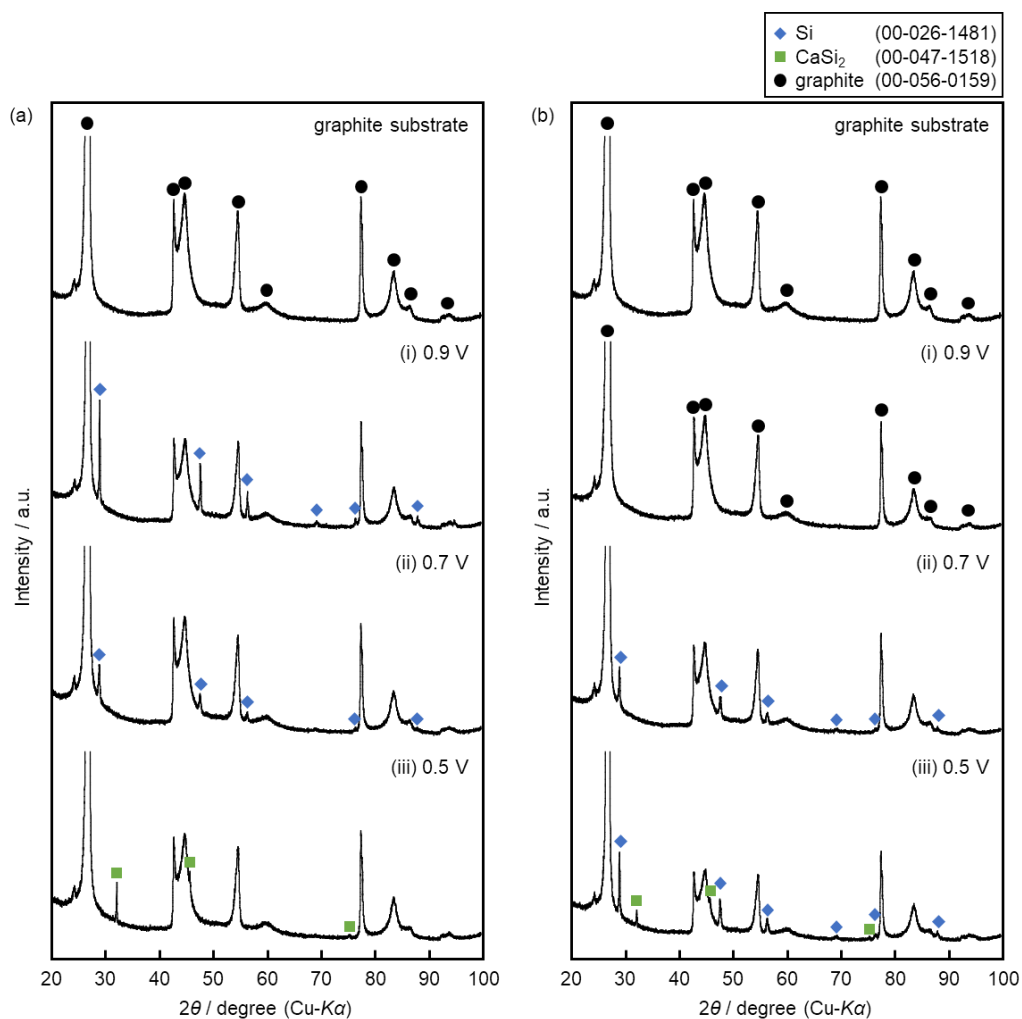
Figure 6. XRD patterns of the graphite substrate and samples obtained by electrolysis at graphite plates in molten NaCl–CaCl$_2$ containing (a) 1.0 mol% of CaSiO$_3$, and (b) 1.0 mol% of CaO and 1.0 mol% of CaSiO$_3$. Charge density: −14 C cm^{-2}.
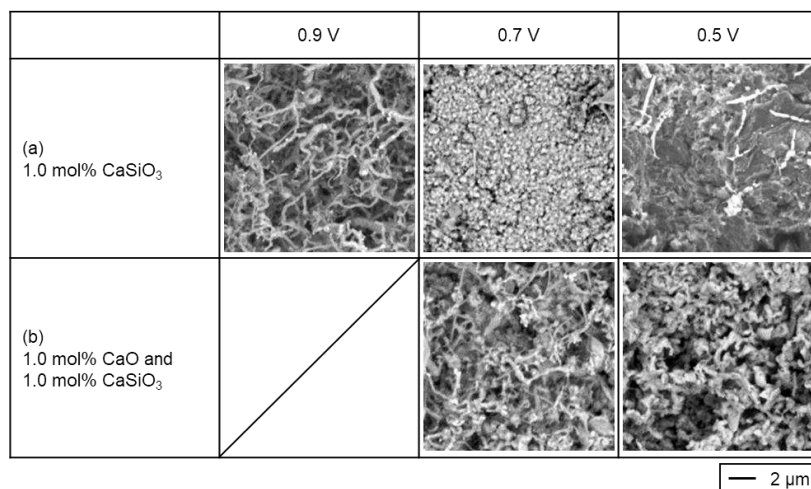

Figure 7. SEM images of the samples obtained by electrolysis at graphite plates in molten NaCl–CaCl$_2$ containing (a) 1.0 mol% of CaSiO$_3$, and (b) 1.0 mol% of CaO and 1.0 mol% of CaSiO$_3$. Charge density: −14 C cm^{-2}.

Conclusion

The structural analysis and electrochemical reduction of silicate ions at the solid graphite substrate were conducted as the preliminary study for liquid Zn cathode. The structure of silicate ions in molten $NaCl$–$CaCl_2$ containing (a) 1.0 mol% of $CaSiO_3$ and (b) 1.0 mol% of CaO and 1.0 mol% of $CaSiO_3$ was investigated by Raman spectroscopy. The main structure is SiO_3^{2-} ion in molten salt (a) and SiO_4^{4-} ion in molten salt (b), which is consistent well with the O^{2-}/SiO_2 ratio in the melts. In molten salt (a), electrodeposition of Si was confirmed at 0.70–0.90 V and formation of $CaSi_2$ at 0.50 V. In molten salt (b), pure Si deposition was only confirmed at 0.70 V and the mixture of Si and $CaSi_2$ was observed at 0.50 V. Thus, SiO_3^{2-} ion is likely to be more suitable for the electrodeposition of Si at liquid Zn cathode as well as at solid graphite electrode.

Acknowledgement

Reference

1. *Industrial Rare Metal 2019*, Arumu Publ. Co. (2019).
2. *Photovoltaic Market 2019*, RTS Corp. (2019).
3. X. Ma, T. Yoshikawa and K. Morita, *Sep. Purif. Technol.*, **125**, 264 (2014).
4. S. Honda, M. Yasueda, S. Hayashida and M. Yamaguchi: Japanese Patent, Toku Kai H19-145663 (2007).
5. T. Nohira, K. Yasuda and Y. Ito, *Nat. Mater.*, **2**, 397 (2003).
6. K. Yasuda, T. Nohira, R. Hagiwara and Y. H. Ogata, *J. Electrochem. Soc.*, **154**, E95 (2007).
7. T. Toba, K. Yasuda, T. Nohira, X. Yang, R. Hagiwara, K. Ichitsubo, K. Masuda and T. Homma, *Electrochemistry*, **81**, 559 (2013).
8. T. Nohira, A. Ido, T. Shimao, X. Yang, K. Yasuda, R. Hagiwara and T. Homma, *ECS Trans.*, **75**(15), 17 (2016).
9. K. Yasuda, T. Shimao, R. Hagiwara, T. Homma and T. Nohira, *J. Electrochem. Soc.*, **164**, H5049 (2017).
10. Y. Ma, A. Ido, K. Yasuda, R. Hagiwara and T. Nohira, *J. Electrochem. Soc.*, **166**, D162 (2019).
11. X. Yang, L. Ji, X. Zou, T. Lim, J. Zhao, E. T. Yu and A. J. Bard, *Angew. Chem. Int. Ed.*, **56**, 15078 (2017).
12. X. Zou, L. Ji, J. Ge, D. R. Sadoway, E. T. Yu and A. J. Bard, *Nat. Commun.*, **10**, 5772 (2019).
13. C. R. Masson, *Jour. Iron Steel Inst.*, **210**, 89 (1972).
14. S. A. Brawer and W. B. White, *Chem. Phys.*, **63**, 2421 (1975).
15. P. Sen and M. Thorpe, *Phys. Rev. B*, **15**, 4030 (1977).
16. F. L. Galeener, *Phys. Rev. B*, **19**, 4292 (1979).
17. H. Verweij, *Jour. Non-Cryst. Solids*, **33**, 41 (1979).